RJ 10191 (95065) June 1, 2000
Engineering and Technology

Research Report

WEAR OF ULTRA-THIN CARBON OVERCOAT CHARACTERIZED BY MICRO-WEAR SCAN AND AUGER ELECTRON SPECTROSCOPY

Tsai-Wei Wu
Vaughn Deline

IBM Almaden Research Center
650 Harry Road San Jose, CA 95120-6099

Thomas Scharf

University of Alabama, the Center for MINT, Dept. Metallurgical and Materials Engineering
Tuscaloosa, AL 35487

Bing K. Yen

IBM Almaden Research Center
650 Harry Road San Jose, CA 95120-6099

John A. Bernard

University of Alabama, the Center for MINT, Dept. Metallurgical and Materials Engineering
Tuscaloosa, AL 35487

RJ 10191 (95065) June 1, 2000
Engineering and Technology

Wear of Ultra-Thin Carbon Overcoat Characterized by Micro-Wear Scan and Auger Electron Spectroscopy

Tsai-Wei Wu*, Vaughn Deline*, Thomas Scharf**, Bing K. Yen* and John A. Barnard**

* IBM Almaden Research Center, 650 Harry Road, San Jose, CA 95120

** University of Alabama, the Center for MINT, Dept. Metallurgical and Materials Engineering, Tuscaloosa, AL 35487

ABSTRACT

A new methodology was developed to characterize the tribological performance of ultra-thin carbon coatings by the micro-wear scan and Auger electron spectroscopy (AES). With the magnetic recording application in mind, two 5 nm-thick carbon coatings were deposited on magnetic disks for the study. In a micro-wear scan process, there were two competing mechanisms that lead to the carbon coating failure — the *coating wear-off* and the *coating structural damage*. The coating wear-off was a continuous process and always being active, whereas the coating structural damage appeared more in a disruptive manner as the applied normal load approached a critical level. The term *coating wear rate,* defined as the coating thickness reduction per unit applied normal load, was adopted in this micro-wear scan test. Two simulation models based on carbon (272 eV) and cobalt (775 eV) Auger electron signals, respectively, were developed to calculate the carbon residual thickness inside the wear track. Because of the difference in signal intensities, the coating residual thickness acquired from the carbon Auger electron signal turned out to be much more robust and reproducible than the cobalt signal. Based on these results, a tribological characteristic chart, which contained both the coating wear rate and critical load parameters, is proposed to offer a better understanding and ranking capability towards the tribological performance of ultra-thin coating systems.

Wear of Ultra-Thin Carbon Overcoat Characterized by Micro-Wear Scan and Auger Electron Spectroscopy

Tsai-Wei Wu*, Vaughn Deline*, Thomas Scharf**, Bing K. Yen* and John A. Barnard**

* IBM Almaden Research Center, 650 Harry Road, San Jose, CA 95120

** University of Alabama, the Center for MINT, Dept. Metallurgical and Materials Engineering, Tuscaloosa, AL 35487

ABSTRACT

A new methodology was developed to characterize the tribological performance of ultra-thin carbon coatings by the micro-wear scan and Auger electron spectroscopy (AES). With the magnetic recording application in mind, two 5 nm-thick carbon coatings were deposited on magnetic disks for the study. In a micro-wear scan process, there were two competing mechanisms that lead to the carbon coating failure — the *coating wear-off* and the *coating structural damage*. The coating wear-off was a continuous process and always being active, whereas the coating structural damage appeared more in a disruptive manner as the applied normal load approached a critical level. The term *coating wear rate*, defined as the coating thickness reduction per unit applied normal load, was adopted in this micro-wear scan test. Two simulation models based on carbon (272 eV) and cobalt (775 eV) Auger electron signals, respectively, were developed to calculate the carbon residual thickness inside the wear track. Because of the difference in signal intensities, the coating residual thickness acquired from the carbon Auger electron signal turned out to be much more robust and reproducible than the cobalt signal. Based on these results, a tribological characteristic chart, which contained both the coating wear rate and critical load parameters, is proposed to offer a better understanding and ranking capability towards the tribological performance of ultra-thin coating systems.

INTRODUCTION

Current micro- and nano-mechanical techniques provide the capability of ranking the mechanical strength of ultra-thin coating systems by utilizing a critical load criterion. However, there is often a lack of correlation between the coating mechanical strength and its tribological performance. It is also generally agreed that in a repetitive contact-sliding environment, for example, the head/disk interface in a hard disk drive, a coating system can fail by gradual wear-off and/or disruptive coating rupturing. In fact, a coating system often fails by the combination of the initial wear-off and the subsequent coating structural damage.

The micro-wear scan technique has the capability to characterize the mechanical strength of an ultra-thin coating system in a repetitive sliding-contact environment [1-3]. In addition to

offering a critical load parameter for ranking the coating strength, the well defined micro-wear tracks generated during the test have been further utilized to study the wear morphology, failure mechanism, and, as discussed in this report, the wear resistance of coatings.

We have investigated the tribological performance of two 5 nm-thick carbon coatings by combining two techniques — the micro-wear scan test and Auger Electron Spectroscopy (AES). First, the micro-wear tester generated 20 μm wide by ~85 μm long wear tracks with a ramped loading condition [1-3]. Because of the ramped loading scheme, the wear-scan was able to preserve the coating morphologies of the initial contact, coating burnishing, thinning down and final catastrophic rupturing. Second, we developed a point-to-point probing routine to measure the carbon and cobalt Auger electron signals across the track length and the virgin surface at each end. Third, we developed two simulation models based on the C and Co Auger electron signals, respectively, to calculate the carbon coating residual thickness inside the wear track. With these steps, we established a comprehensive methodology that allowed us to quantify the wear of carbon coating as thin as 5 nm.

Based on our findings, we propose a tribological characteristic chart, which contains the coating wear rate and wear-scan critical load information, to represent the coating tribological behavior. This chart offers not only a better understanding in the coating failure mechanism but also criteria in ranking the coating tribological performance.

EXPERIMENTAL

Sample preparation

Using a capacitively coupled RF plasma beam source [4, 5], 5 nm-thick carbon coatings were deposited on magnetic disk media, which consisted of Al-Mg substrate coated with NiP/Cr/CoCrPt layers. Mixtures of C_2H_2 and N_2 were used as source gases to produce amorphous carbon films. The chamber pressure was maintained at 0.5mTorr during deposition. Two coating systems, denoted as Samples IB4 and IB9, were selected as a model set for this study because of their distinctive mechanical properties in terms of their critical loads [6] and micro-hardness (ref. Table I).

Table I. The mechanical properties of the model sample set

Sample ID	H (at.%)	N (at.%)	Hardness[1] (GPa)	Critical load[2] (mN)	Wear rate[3] (Å/mN)
IB4	10	25	18	11	1.2
IB9	27	0	25	9	1.8

1. The hardness was measured independently by using the nano-indentation technique on the same types of coatings but with a 100nm thickness and on Si substrates.

2. The critical load was measured by the micro-wear scan technique.
3. Coating wear rate here is defined as the coating thickness reduction per unit applied normal load. Further details are discussed in this report.

Micro-wear scan technique

Fig. 1 shows the schematic of the micro-wear tester [1-3]. A diamond conical indenter with a nominal tip radius of ~5 μm was employed. In the course of a micro-wear scan, the sample scans at a speed of 0.18 μm/sec along the Y-direction while the indenter is oscillating at a frequency of ~6.55 Hz along the X-direction. At the same time, the indenter was being pushed toward the coating surface to gradually increase the normal loading. Furthermore, assuming that there is a 1 μm^2 or larger contact area made by the indenter, then as the indenter scans across any given point on the surface, there are at least 73 wear passes over this material point. Therefore, a fatigue characteristic has been built into the wear-scan testing scheme.

Because the micro-wear scan is capable of creating a 20 μm wide by ~85 μm long wear track and preserving the wear morphology inside the track, this unique feature facilitates many ex-situ surface analyses, including the AES routine described in the following session.

Auger Electron Spectroscopy

The Auger electron spectroscopy measurements were obtained with a Physical Electronics 600 scanning Auger microprobe. A 3 kV electron beam of approximately 100 nA was utilized. The beam diameter is less than 1μm. Physical Electronics' Spec View software was used to measure the line scans of the carbon at 272 eV and cobalt at 775 eV Auger transitions. Measurements were spaced every 1 μm over a total distance of 200 μm. The line scans were acquired over a 1 hour time period with the cobalt signal being measured three times as long as the carbon signal to improve the measurement statistics of the weaker cobalt signal.

Coating Thickness Simulation Model

Two carbon thickness simulation models were developed for analyzing the carbon (272 eV) and cobalt (775 eV) Auger electron signals, respectively. Based on the Beer's attenuation law, the inelastic mean free path of electrons in the carbon coating, and the disk coating configuration, each model is capable of extracting the residual carbon thickness from the measured Auger signals.

Model 1: Simulation model based on cobalt Auger signal (Co, $E = 775\ eV$)

Assuming that the Co Auger signal measured at the C/Co-alloy interface is I_o for the coating configuration shown in Fig. 2a, then the signal should drop to $I(t) = I_o e^{-t/\lambda}$ at the free surface. Where t is the residual carbon coating thickness and λ is the inelastic mean free path of the

electrons in the carbon coating. By normalizing the signal $I(t)$ by the signal measured from the virgin area $I(t_o) = I_o e^{-t_o/\lambda}$, the normalized Co Auger electron intensity can be expressed as

$$\ln\frac{I(t)}{I(t_o)} = -\frac{(t-t_o)}{\lambda} \qquad [1]$$

Then the carbon thickness loss Δt is

$$\Delta t = t_o - t = \lambda \ln\frac{I(t)}{I(t_o)} \qquad [2]$$

where t_o is the original carbon thickness.

Model 2: Simulation model based on carbon Auger signal (C, E = 272 eV)

Assuming that the yield of carbon Auger electrons per volume element inside the carbon coating is i_o, as schematically shown in Fig. 2b, then the carbon Auger electrons generated from the disk-shaped volume element Adz at position z is $i_o Adz$. Among them, those that are capable of escaping to the free surface are

$$dI(t) = e^{-(t-z)/\lambda} i_o A dz \qquad [3]$$

where A is the cross-section area of the volume element and λ now is the carbon Auger electron's inelastic mean free path in the carbon coating. Therefore, the total carbon Auger electrons that are generated from the carbon volume $(A \cdot t)$ and also escaping to the free surface are

$$I(t) = \int_0^t e^{-(t-z)/\lambda} i_o A dz = i_o A\lambda(1-e^{-t/\lambda}) \qquad [4]$$

Then the normalized C Auger intensity is

$$\frac{I(t)}{I(t_o)} = \frac{(1-e^{-t/\lambda})}{(1-e^{-t_o/\lambda})} \qquad [5]$$

After rearranging Eq. 5, the carbon thickness reduction, Δt, can be expressed as

$$\Delta t = t_o - t = \lambda \ln[\beta(1-(1-\frac{1}{\beta})\frac{I(t)}{I(t_o)}] \qquad [6]$$

where $\beta = e^{t_o/\lambda}$.

Eqs. 2 and 6 will be employed to convert the measured Co and C Auger signals, respectively, to the carbon coating thickness reduction.

RESULTS

Fig. 3 shows the compiled results acquired from the micro-wear scanning, SEM morphological imaging, and coating surface profiling by Tencor® profilometry. A more elaborate data interpretation of the results will be discussed elsewhere [6]. In this study, we are focusing on the coating wear which occurred in the micro-wear scan process. It is apparent from Figs. 3b and 3c that in the early stage of the wear process, where the applied normal load is below the critical level, the wear morphology shows the surface features, including coating burnishing, texture line polishing, etc., but no catastrophic types of coating failures. The wear surface still remains uniform and smooth, although there is some carbon material loss.

Fig. 4b schematically illustrates how an Auger scan measurement is implemented along the wear track of IB9 coating. Because the Auger probing length is deliberately chosen to be 200 μm, it not only fully covers the entire track length of ~85 μm but also provides two baseline references measured from the virgin areas at the track ends. The baseline signal level is used for the signal normalization in the model simulation. With an electron beam spot size of ~1 μm and a probing spacing of 1 μm, the point-to-point Auger signals form a continuous Auger signal profile across the entire wear track. This is illustrated in Fig. 4a, where the C and Co signal profiles of an IB9 track are plotted together with the apparent friction coefficient (*FR*) curve [6]. Furthermore, since all the key devices involved have a sub-micron precision in position control, the measured Auger signal can be easily correlated to the micro-mechanical data (Fig. 3a), wear morphology (Fig. 3b), and the surface roughness (Fig. 3c) through the common track length axis. Fig. 5 shows another example of the Auger signal profiles acquired from a different IB9 track, where the carbon, cobalt, and oxygen elemental signal profiles are superimposed together but not in scale.

Fig. 6a shows the IB4 and IB9 carbon thickness reduction curves by using the C Auger electron model (from Eq. 6). Fig. 6b basically shows the same information but using the Co Auger model (from Eq. 2). The parameters t_o = 5 nm and λ = 15 Å were used in the calculations of both models. Furthermore, in Figs. 6a, 6b, and 6c, the applied normal load (*LC*) was chosen to be the common axis for better data presentation.. The axis conversion is made through the *LC vs. scan distance* (*SD*) relation acquired from that particular micro-wear track (ref. the curve denoted by *LC* in Fig. 3a).

Figs. 6a and 6b both show a gradual increase of the carbon coating thickness loss with increasing applied normal load. It is apparent that IB9 carbon coating shows a significant higher thickness reduction rate compared to IB4. Fig. 6c shows the apparent friction coefficient (*FR*) curves of the two samples. It is worthwhile to compare the *FR*-curves with the thickness reduction curves: the friction curves of the IB4 and IB9 carbon coatings start to deviate from each other at the applied load of ~6 mN. Interestingly, the two thickness reduction curves also start to show a major deviation at the same loading. This observation seems to be consistent with the prediction of Archard's empirical law of wear [7], which states that the wear volume is proportional to the normal applied load when other parameters, including the friction coefficient, are held fixed. Therefore, as shown in Fig. 6, under the same normal loading condition, IB9's higher friction coefficient indicates that a higher tangential force was generated during the wear, and it is consistent with the higher rate of the IB9 carbon coating removal.

DISCUSSION

Data Reproducibility and Robustness

While the integrity of the Auger data depends on skillful operation, sample cleanliness and sufficient measurement statistics, there are still inherit limitations associated with the modeling that need to be considered. First, the two simulation models are built up in a relative-scale basis, and therefore, the original coating thickness used in the models has to be accurate in order to ensure the validity of the calculated result, especially the coating thickness loss. Second, the inelastic mean free path adopted in both models should be treated as a fitting parameter rather than an intrinsic physical property. The selection of λ value in the models was not based on the Auger electron energy [8]. Instead, we chose an empirical value of 15 Å in both models, which was obtained through the calibration by X-ray reflectivity in a previous study [9].

In order to check the data reproducibility of the Auger measurements, several Auger scans were performed on the five wear tracks randomly selected from a total of 13 IB9 wear tracks. Figs. 7a and 7b show, respectively, the collections of these C and Co signal profiles. Furthermore, Figs. 8a and 8b show the corresponding carbon thickness reduction curves after working through the models. It is interesting that, as shown in Fig. 8a, although the five raw C signal profiles look quite different and very scattered in terms of their signal ranges and baseline levels, the resulting thickness reduction curves are reasonably convergent and reproducible.

Unfortunately, the Co signal profiles do not show the same "data robustness" as the C profiles. As indicated in Fig. 8b, the thickness reduction curves derived from the Co profiles are very sensitive to the individual baseline level. Since the Co signal intensity is much lower than the C signal and is near the signal noise background of the Auger spectrometer, the measured Co baseline has a larger error than the C baseline. In fact, only those Co profiles that share similar baseline levels render convergent thickness results. For those Co profiles that have different baseline levels, the thickness reduction curves become scattered and, sometimes, the thickness reduction values are so far off that the results become meaningless.

The fact that the C Auger signal is much more robust than the Co signal may be due to the following reason: because there is a signal normalization step embedded in the models, i.e., the $I(t)/I(t_o)$ term in both Eqs. 2 and 6, the data robustness depends on the *ratio* of *signal range* to *baseline level* and generally the smaller the ratio the more robust the calculated result. For both IB4 and IB9 carbon coating systems, the Co signal is at least an order of magnitude lower than the C signal. Also, the Co baseline level sometimes is in the vicinity of the system's background noise, whereas the C level is around ~30K counts in average. In comparison, the Co signal profile has the ratio ranging from 4 to 120, and the ratio of the C signal profile is around ~0.3 in average.

Consistency between the Two Simulation Models

If we only select those three Co signal profiles (Fig. 7b) that share the same baseline levels for the Co model simulation and use $\lambda = 15$ Å, the resulting thickness reduction curves are plotted in Fig. 9 together with their C signal counterparts. The two sets of thickness results are reasonably consistent with each other and so is the data reproducibility. In fact, there are at least two extrinsic variables capable of interfering and suppressing the Co signal: First, the Co Auger electrons in average travel through a longer distance than the C Auger electrons in order to reach the free surface. Second, whenever the 5 nm carbon coating is thinned down to or below ~2 nm during the wear scan, a thin Co-oxide layer is rapidly formed along the C/Co-alloy interface [9, 10]. This Co oxide layer clearly changes the coating configuration and, as a result, invalidates the current Co model. Apparently, the Co oxide layer does not influence the carbon model.

Tribological Characteristic Chart—A New Way to Represent Coating Wear Properties

Because of the simple coating configurations adopted in the models (Figs. 2a and 2b), it is important to realize that the coating thickness data is only valid and applicable over the so-called *smooth wear-off portion* of a wear track. Any coating structural damage in addition to the on-going coating wear would introduce complexities and ambiguities to the Auger measurement and hence the data interpretation, even if the thickness reduction curve apparently continues the trend extended from the uniform wear regime.

A tribological characteristic plot of the ultra-thin coating system can be constructed by the following steps: 1) plotting the *coating residual thickness vs. applied normal load (LC)* curve and 2) truncating the curve at the corresponding critical load and re-set the remaining coating thickness to zero. As an example, the tribological characteristic plots of the IB4 and IB9 coatings are illustrated in Fig. 10, in which we have utilized the thickness reduction data from Fig. 6a and the micro-wear scan critical loads listed in Table I.

Furthermore, if we define the terminology *coating wear rate* as the *coating thickness reduction per unit normal applied load*, we thus enable another useful parameter in addition to the critical load to evaluate the tribological performance of ultra-thin coating systems. For instance, in Fig. 10, the slope of the residual coating thickness curve represents the *coating wear rate* and the curve truncation indicates where the coating *structure* is severely *damaged*. It is clear from Fig. 10 that the IB4 carbon coating is the superior protective coating because of its lower wear rate and higher critical load. In fact, IB4 coating indeed showed a better performance in the

functional contact-start-stop test than IB9. Similar results have been reported for the sputtered carbon coating by Wei et al. [11]. They observed that 10 nm thick sputtered a-C:N overcoats with nitrogen contents of 12-20% exhibited better wear resistances and lower friction coefficients over the undoped a-C coating.

In theory, the wear resistance and critical load do not have to correlate with each other. For example, if two coating systems have hypothetical tribological characteristics shown in Fig. 11, then the choice of overcoat would critically depend on the loading condition. If the equivalent asperity impact would always be lower than L_{cr1} under the normal loading condition, then Carbon 1 should be a better choice because of its relative lower wear rate and hence a longer lifetime. However, if the contact condition is very erratic and occasional high load impacts do exist, then Carbon 2 might be the better choice because of its higher critical load and impact toughness to prevent disruptive coating failures. Therefore, it is important to understand the functional environment and find out the dominant driving mechanism that leads to the ultimate failure of the coating system when selecting proper protective coatings.

In summary, we have illustrated a more comprehensive micro-mechanical characterization methodology that has the potential in linking mechanical properties to tribological performance of ultra-thin coating systems. By quantifying the actual wear of the 5 nm-thick carbon coatings, we have confirmed our previous assumption about the coating failure mechanisms occurring in the micro-wear process. The proposed coating characteristic plot, i.e. the residual coating thickness curve truncated at the corresponding critical load, offers two important parameters — the wear rate and critical load — to better rank the coating tribological performance.

CONCLUSIONS

- We have successfully developed a new methodology by combining the micro-wear scan technique and Auger electron spectroscopy to investigate the tribological behavior of 5 nm-thick carbon coatings.
- Two Auger electron simulation models, which are based on the Beer's attenuation law, coating configuration, and Auger electron's inelastic mean free path, are developed and successfully applied in the calculation of the residual carbon coating thickness.
- Because of the substantial difference in the Auger signal intensities, the coating thickness result acquired from the carbon Auger profile is much more robust and reproducible than that from the cobalt signal profile.
- In the micro-wear scan process, there are always two competing mechanisms that lead to the ultimate coating failure, namely, the *coating wear-off* and the *coating structural damage*. The coating wear-off is a continuous process and always active in the wear-scan process, whereas the coating structural damage sets in disruptively when the applied normal load approaches a critical level.
- A tribological characteristic chart, comprising a residual coating thickness curve and a truncation at the matching critical load, is proposed to better understand and rank the tribological performance of ultra-thin coating systems.

ACKNOWLEDGMENTS

The authors would like to thank Dr. H. Zhang of IBM Storage Technology Division (STD) and D. Miller of IBM Almaden Research Center (ARC) for their stimulating discussion on AES and other surface analysis techniques, Dr. R. L. White of IBM STD for measuring the carbon hardness, Dr. J.-U. Thiele of IBM STD and Dr. M. Geisler of BPS Inc. for their assistance in sample preparation. The authors also gratefully acknowledge Dr. B. Marchon and Dr. J. Eyerla of IBM ARC for their support and encouragement during the course of this work.

REFERENCES

1. T.W. Wu, in *Thin Films: Stresses and Mechanical Properties V*, edited by S.P. Baker, C.A. Ross, P.H. Townsend, C.A. Volkert, and P. Borgesen (Mater. Res. Soc. Symp. Proc. **356**, Pittsburgh, PA, 1995), p. 755.
2. T.W. Wu and J. Frommer, in *Fundamentals of Nanoindentation and Nanotribology*, edited by N.R. Moody, W.W. Gerberich, N. Burnham, and S.P. Baker, Mater. Res. Soc. Symp. Proc. **522**, Pittsburgh, PA, 1998), p. 287.
3. T.W. Wu, Thomas W. Scharf, Hong Zhang, and John A. Barnard, to be appeared in Mat. Res. Soc. Symp. Proc. **593** (1999).
4. H. Oechsner and B. Tomcik, Surf. Coating Technol., **47**, 162 (1991).
5. M. Weiler, S. Sattel, K. Jung, H. Ehrhardt, V. S. Veerasamy, and J. Robertson, Appl. Phys. Lett., **64**, 2797 (1994).
6. T.W. Scharf, T.W. Wu, B.K. Yen, B. Marchon, and J.A. Barnard, in process.
7. J. Halling, ed., "Principles of Tribology", The Macmillan Press, Ltd., 1978.
8. D. Briggs and M.P. Seah, ed., "Practical Surface Analysis by Auger and X-ray Photoelectron Spectroscopy", John Wiley and Sons, Ltd., 1983.
9. C.M. Mate, B.Y. Yen, D. C.Miller, and M.F. Toney, to be published on IEEE Trans. Magn.
10. M.K. Puchert, P.Y. Timbrell, R.L. Lamb, and D.R. McKenzie, J. Vac. Sci. Technol. A **12**, 727(1994).
11. B. Wei, B Zhang, and K.E. Johnson, J. Appl. Phys., **83**, 2491(1998)

FIGURE CAPTIONS

Fig. 1: The schematic of the micro-wear scan operation.

Fig. 2: (a) The coating configuration of the cobalt (Co) Auger signal model. Notice that I_o is the Co Auger signal measured at the C/Co-alloy interface and $I(t)$ is the signal

measured at the free surface. (b) The coating configuration of the carbon (C) Auger signal model. Notice that i_o is the C Auger signal intensity generated from a unit volume of the carbon material.

Fig. 3: The compiled data set obtained from the micro-wear scan technique and post-surface analyses. (a) The micro-mechanical data plot. The plot comprises the applied normal load (*LC*), tangential force (*TG*) and apparent friction coefficient (*FR*) curves. (b) The corresponding SEM wear morphology and (c) track surface profile.

Fig. 4: (a) The superposition of the C, Co Auger signal profiles (i.e., denoted by the C and Co signals) and apparent friction coefficient (*FR*) curve. (b) Schematically illustrating how an Auger scan is implemented along a wear track. Where the Auger probing length was 200μm and the probing interval was 1μm. Notice that the Auger scan covers the unworn areas at both track ends.

Fig. 5: The superposition the C and Co Auger signal profiles obtained from the IB9 carbon coating. Notice that the oxygen signal profile, which is generated from the Co-oxide layer along the C/Co-alloy interface, is also included. All three signal profiles are plotted in arbitrary units.

Fig. 6: The comparison of the coating thickness reduction curves between IB9 and IB4: In (a), the curves are derived by using the carbon model, and in (b), by the cobalt model. In (c), the plot shows the apparent friction coefficient (*FR*) curves of IB9 and IB4. Notice that, in these three plots, the deviations between IB4 and IB9 are all starting at *LC*=~6mN.

Fig. 7: Collections of (a) the C and (b) Co Auger signal profiles. Notice that the C signal is at least an order of magnitude larger than that of Co, and the baseline level of the C signal is also much higher.

Fig. 8: (a) The carbon coating thickness reduction curves derived from the C signal profiles shown in Fig. 7a. (b) The carbon coating thickness reduction curves derived from the Co signal profiles shown in Fig. 7b. Notice that the curve derived from the C signal is much more robust and reproducible than those derived from the Co signals.

Fig. 9: The superposition of IB9's coating thickness reduction curves obtained from Figs. 8a and 8b. Where only those Co Auger profiles that have similar baseline levels were selected for plotting. Notice that there is a reasonable agreement, particularly before the critical load, between the two models. Furthermore, because of the formation of the Co-oxide layer, the two sets of thickness reduction curves start to deviated at the higher loading regime.

Fig. 10: The tribological characteristic plots of IB4 and IB9 coatings. Each characteristic curve comprises the residual carbon coating thickness curve and the curve truncation at the corresponding critical load. The slope of the thickness curve reflects the coating wear resistance and the truncation location indicates the limit of validity of the wear rate data.

Fig. 11: A scenario of the tribological performances of two imaged coatings. Because there are two characteristic parameters involved in the tribological ranking process, i.e. the coating wear rate and critical load, it depends on the functional loading condition to select the better-suited protective coating.

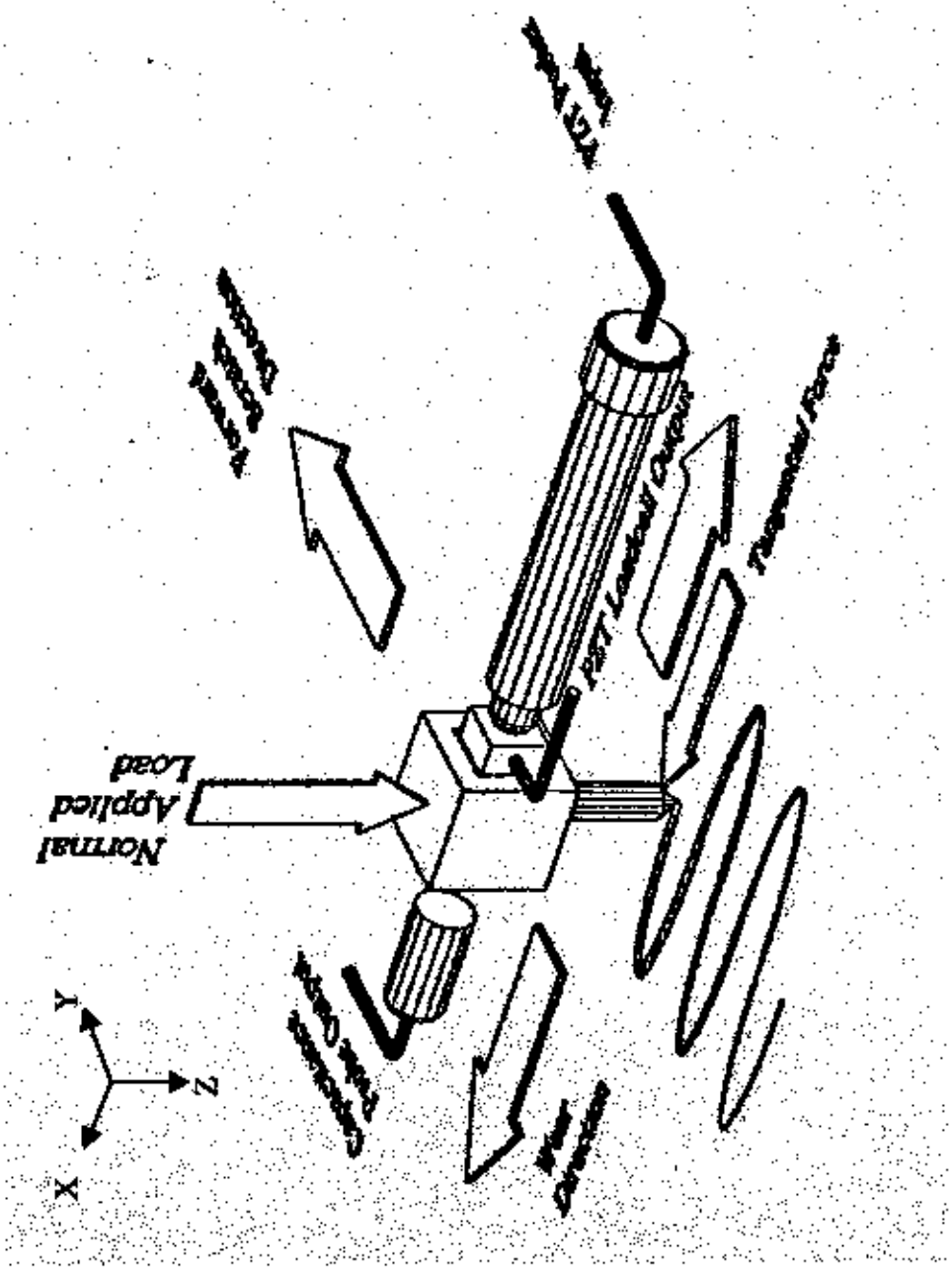

Fig. 1

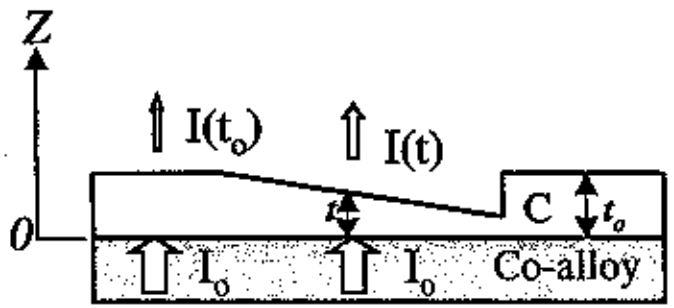

Fig. 2a

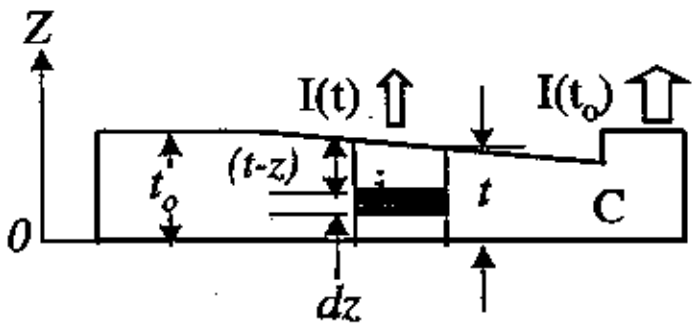

Fig. 2b

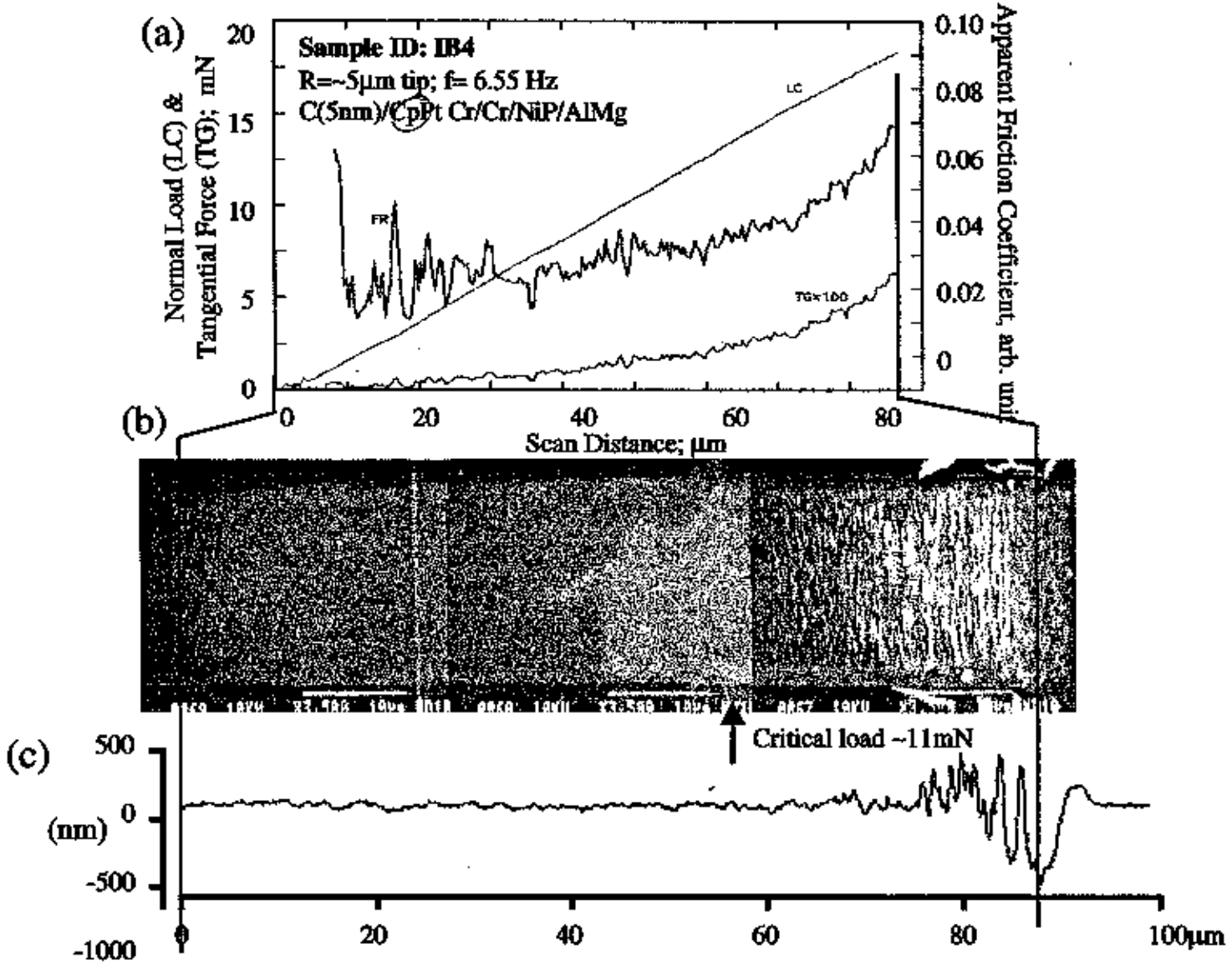
(a)
Sample ID: IB4
R=~5µm tip; f= 6.55 Hz
C(5nm)/CpPt Cr/Cr/NiP/AlMg
Normal Load (LC) & Tangential Force (TG); mN
Apparent Friction Coefficient, arb. uni
LC
FR
TG×100
Scan Distance; µm
(b)
Critical load ~11mN
(c)
(nm)
100µm

Fig. 3

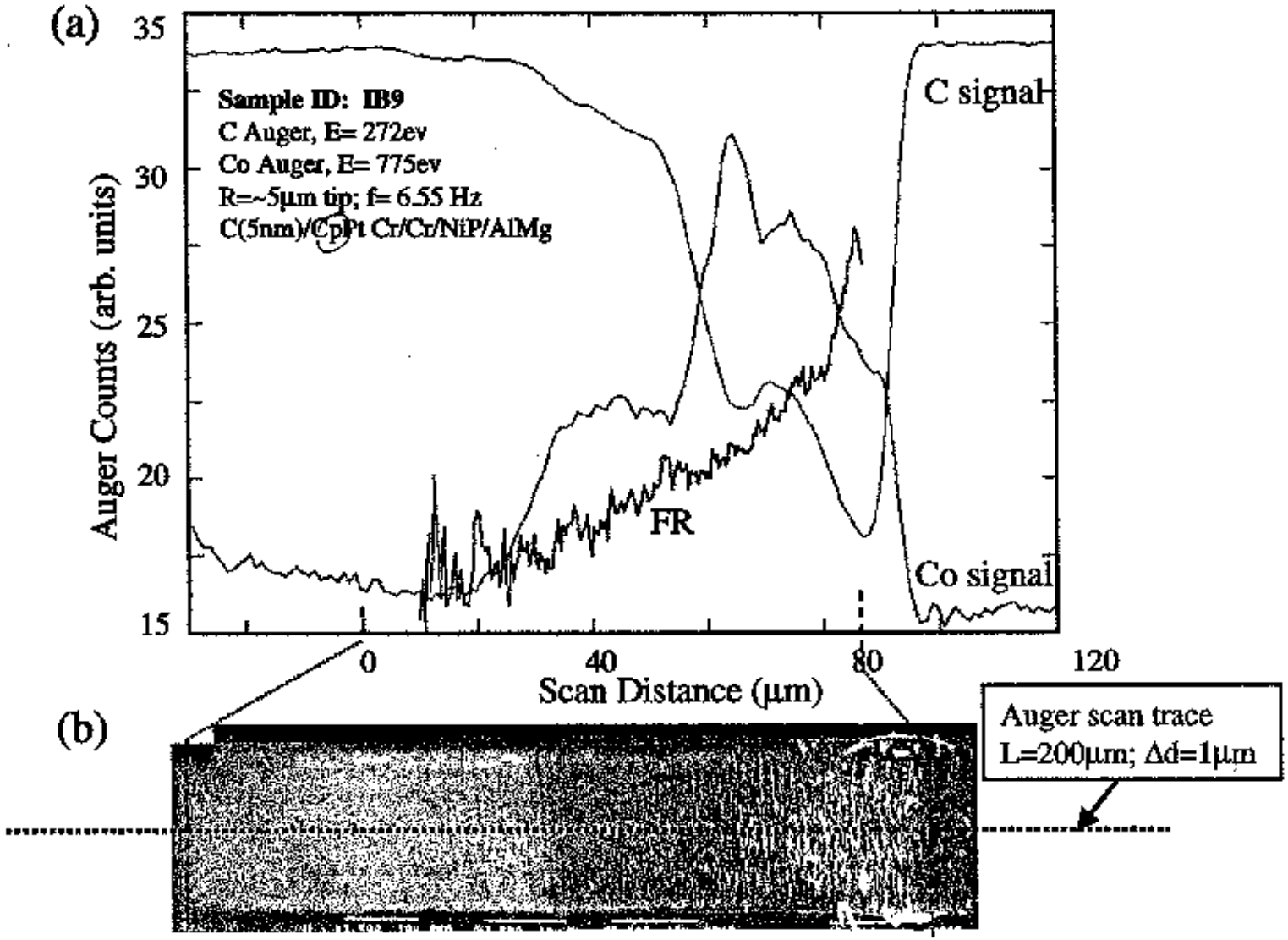
(a)
Sample ID: IB9
C Auger, E= 272ev
Co Auger, E= 775ev
R=~5μm tip; f= 6.55 Hz
C(5nm)/CpPt Cr/Cr/NiP/AlMg
C signal
Co signal
FR
Auger Counts (arb. units)
35
30
25
20
15
0
40
80
120
Scan Distance (μm)
(b)
Auger scan trace
L=200μm; Δd=1μm

Fig. 4

IB6AE01

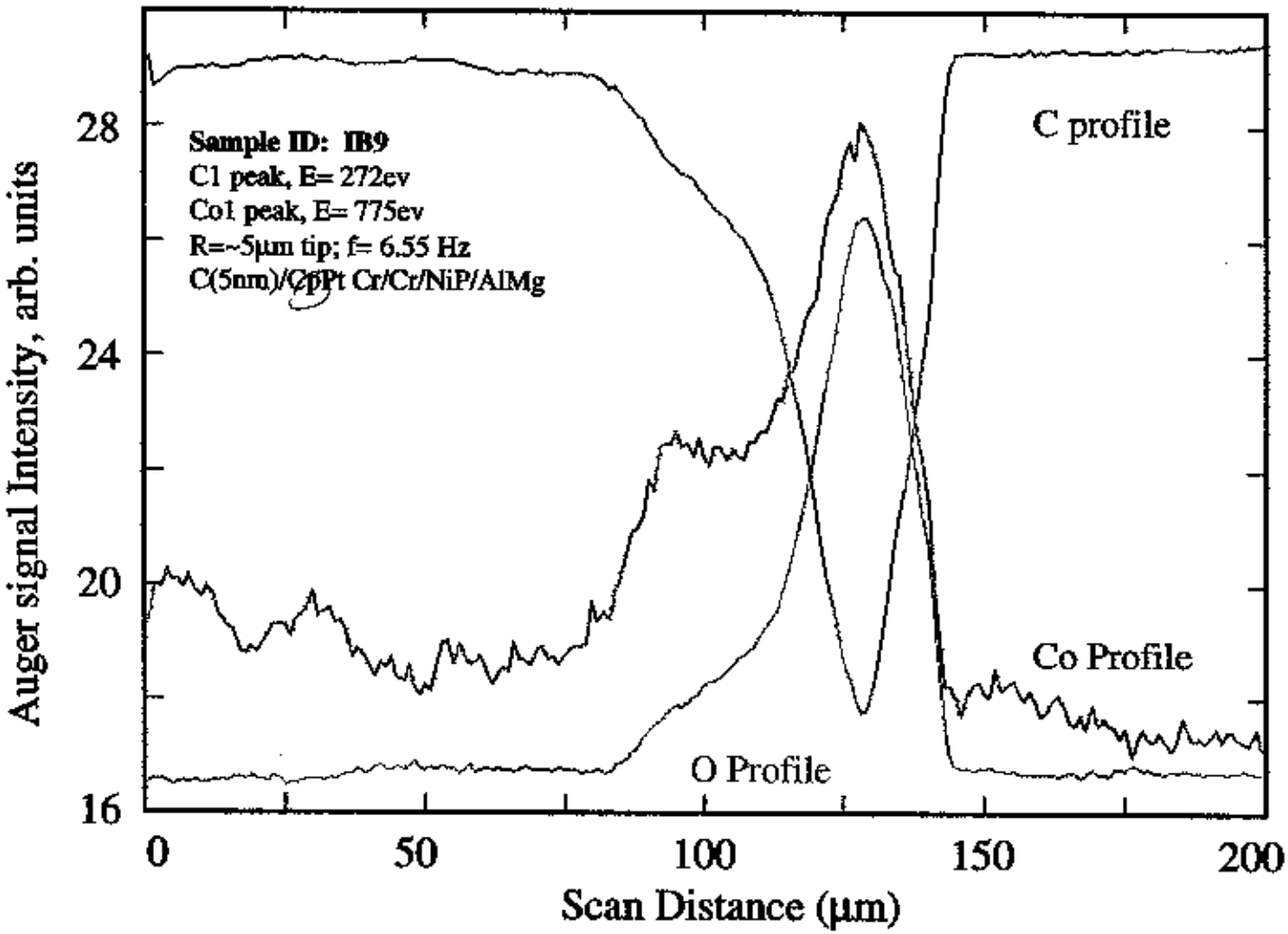

Fig. 5

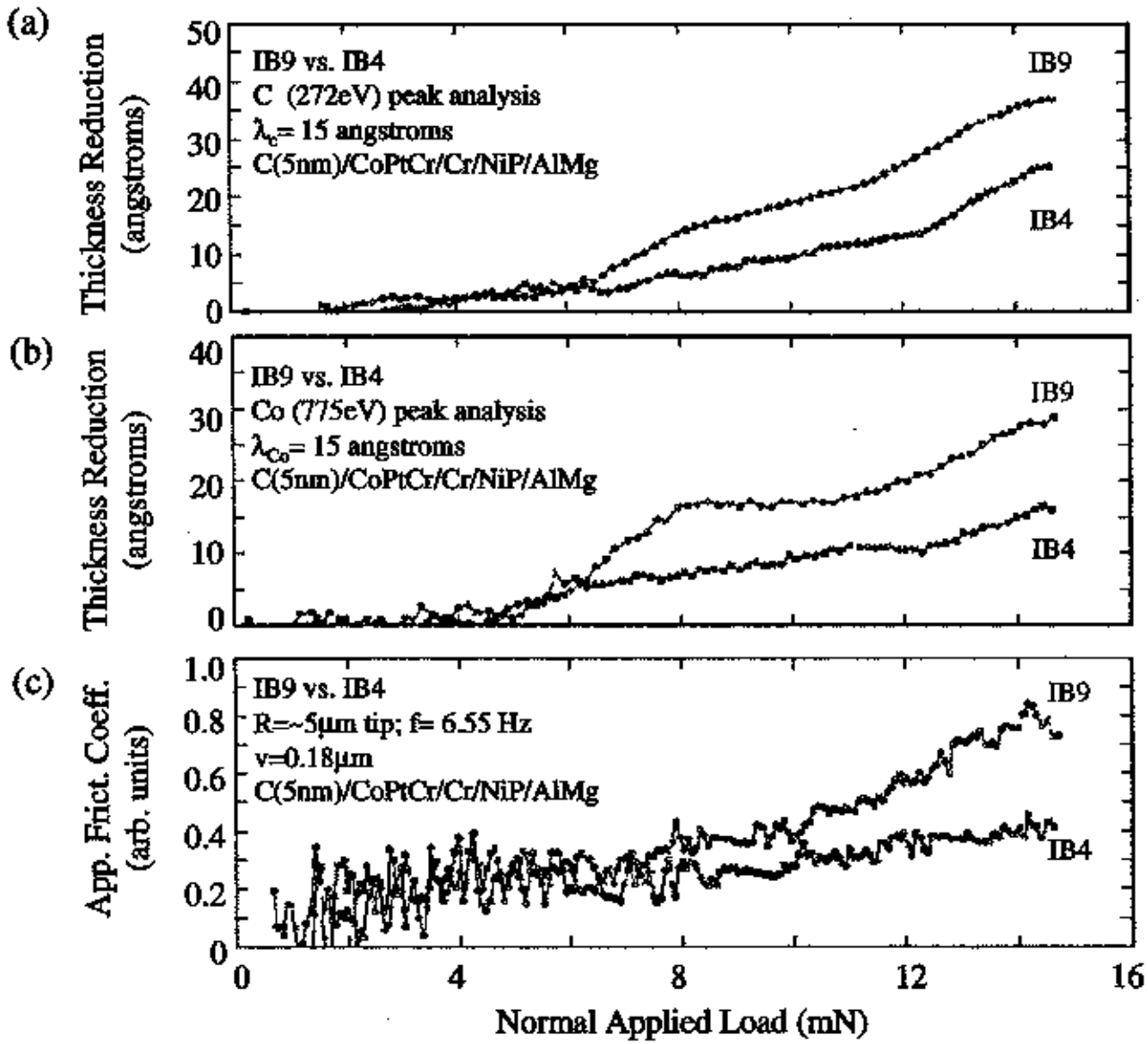
(a)
Thickness Reduction (angstroms)
IB9 vs. IB4
C (272eV) peak analysis
λ_c= 15 angstroms
C(5nm)/CoPtCr/Cr/NiP/AlMg
IB9
IB4
(b)
Thickness Reduction (angstroms)
IB9 vs. IB4
Co (775eV) peak analysis
λ_{Co}= 15 angstroms
C(5nm)/CoPtCr/Cr/NiP/AlMg
IB9
IB4
(c)
App. Fric. Coeff. (arb. units)
IB9 vs. IB4
R=~5μm tip; f= 6.55 Hz
v=0.18μm
C(5nm)/CoPtCr/Cr/NiP/AlMg
IB9
IB4
Normal Applied Load (mN)

Fig. 6

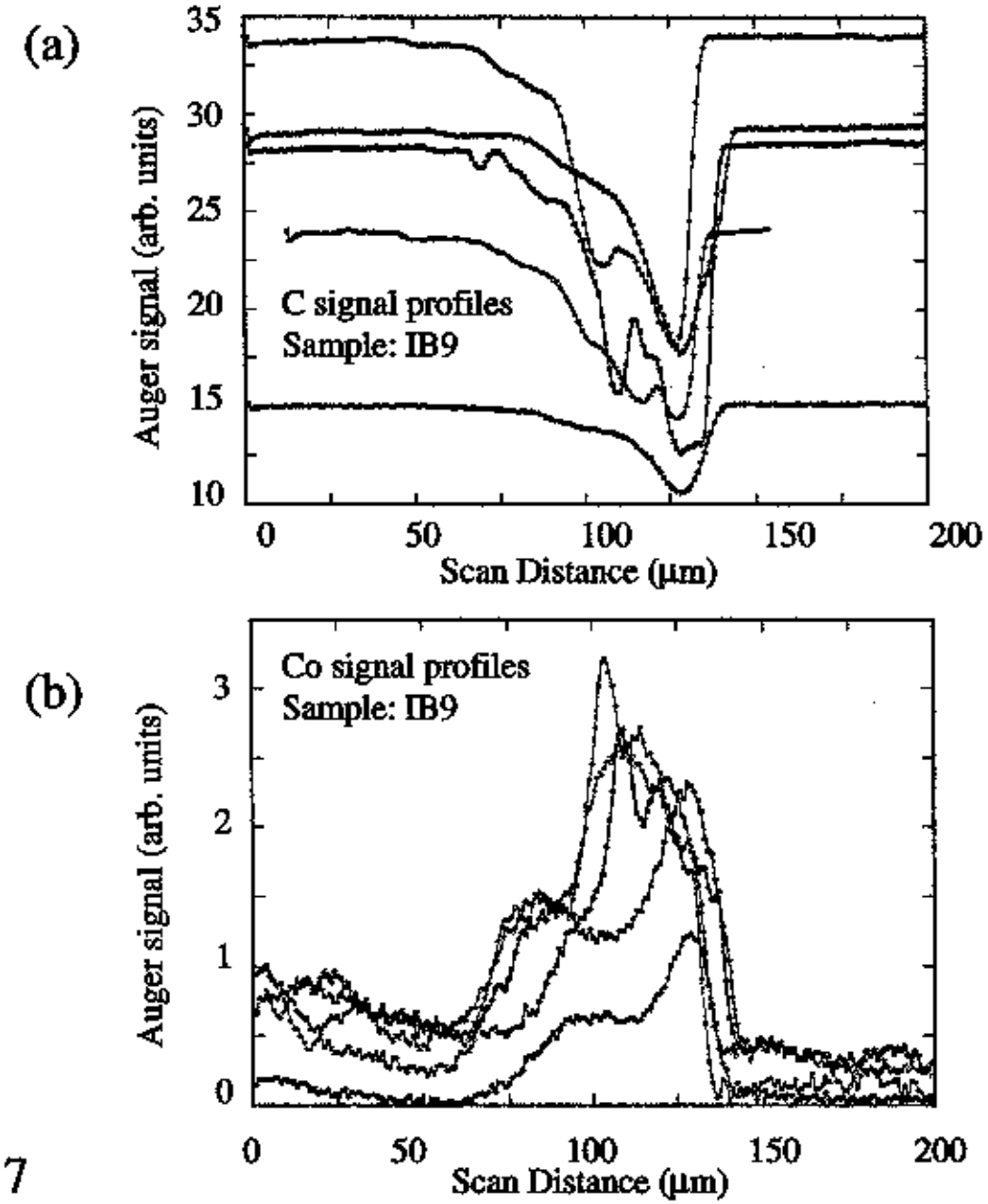
(a)
Auger signal (arb. units)
C signal profiles
Sample: IB9
Scan Distance (μm)
(b)
Co signal profiles
Sample: IB9
Auger signal (arb. units)
Scan Distance (μm)

Fig. 7

(a)

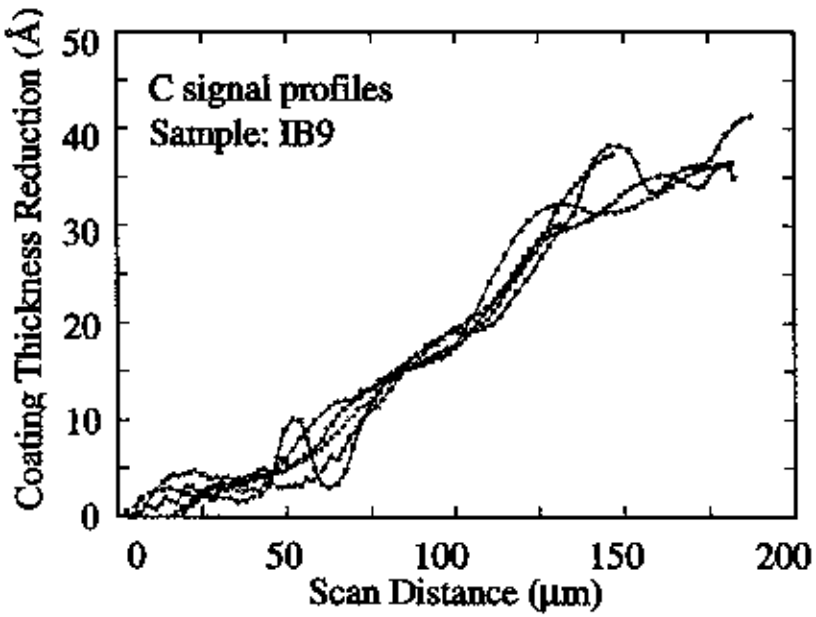
C signal profiles
Sample: IB9
Coating Thickness Reduction (Å)
Scan Distance (μm)
0
10
20
30
40
50
0
50
100
150
200

(b)

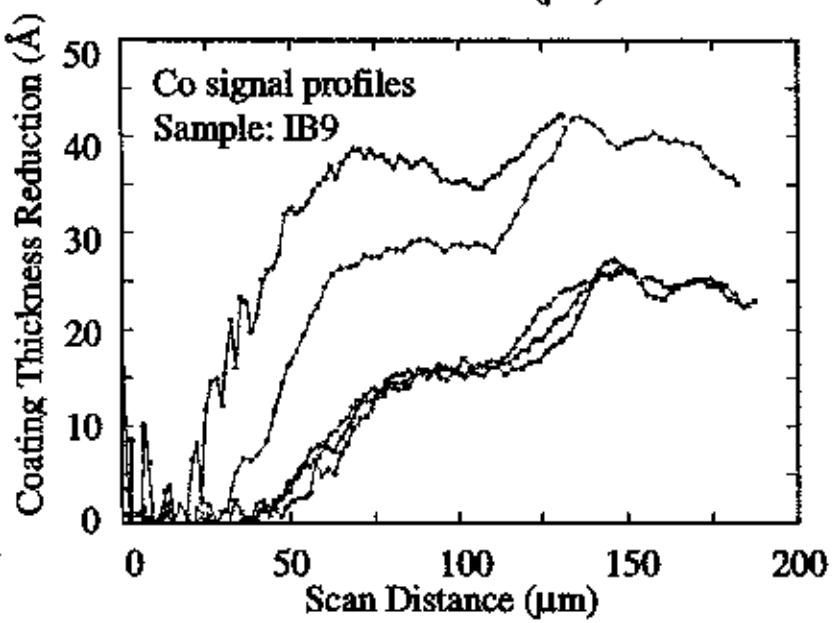
Co signal profiles
Sample: IB9
Coating Thickness Reduction (Å)
Scan Distance (μm)
0
10
20
30
40
50
0
50
100
150
200

Fig. 8

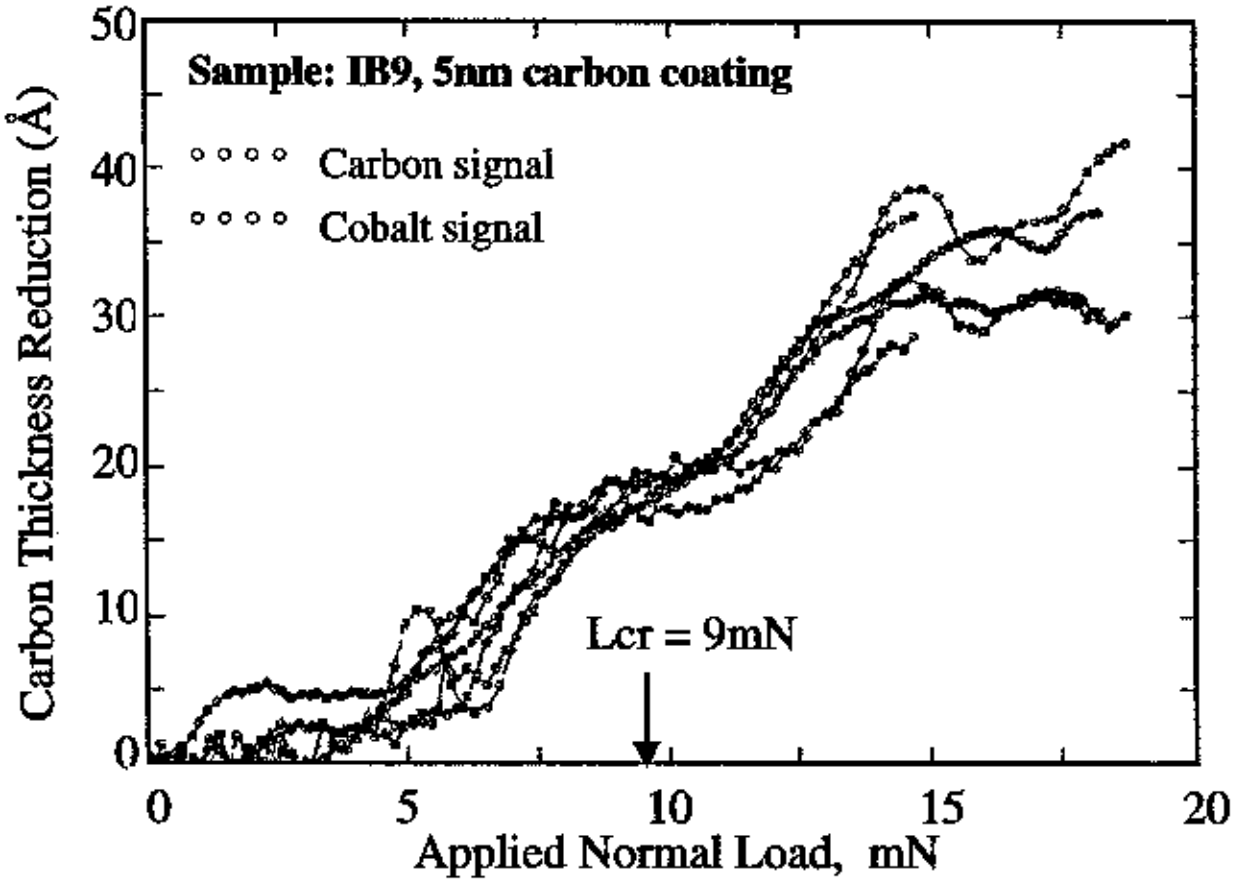
Sample: IB9, 5nm carbon coating
Carbon signal
Cobalt signal
Lcr = 9mN
Carbon Thickness Reduction (Å)
Applied Normal Load, mN
0
10
20
30
40
50
0
5
10
15
20

Fig. 9

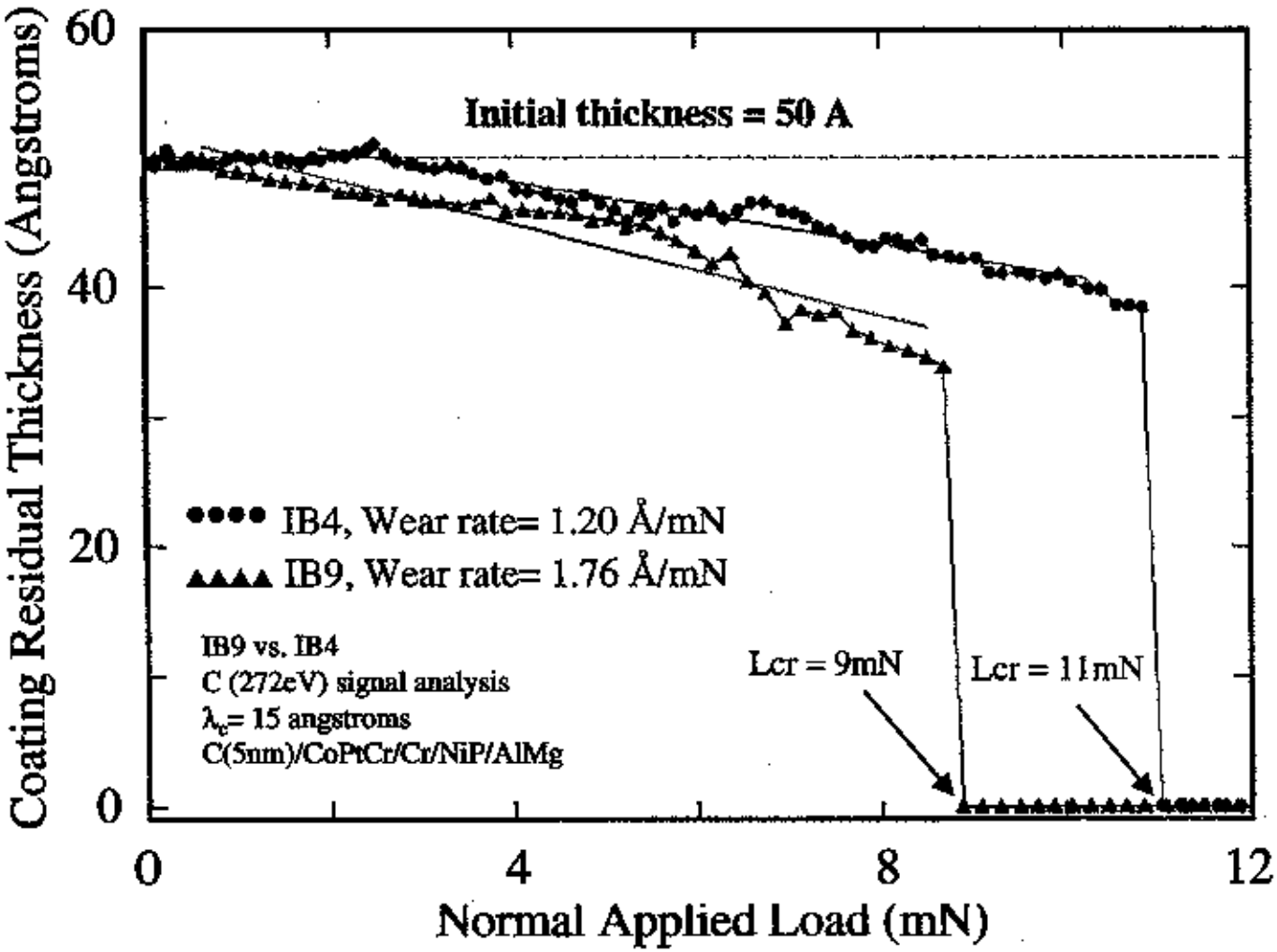
Initial thickness = 50 A
●●●● IB4, Wear rate= 1.20 Å/mN
▲▲▲▲ IB9, Wear rate= 1.76 Å/mN
IB9 vs. IB4
C (272eV) signal analysis
λc= 15 angstroms
C(5nm)/CoPtCr/Cr/NiP/AlMg
Lcr = 9mN
Lcr = 11mN
Coating Residual Thickness (Angstroms)
Normal Applied Load (mN)
0
20
40
60
0
4
8
12

Fig. 10

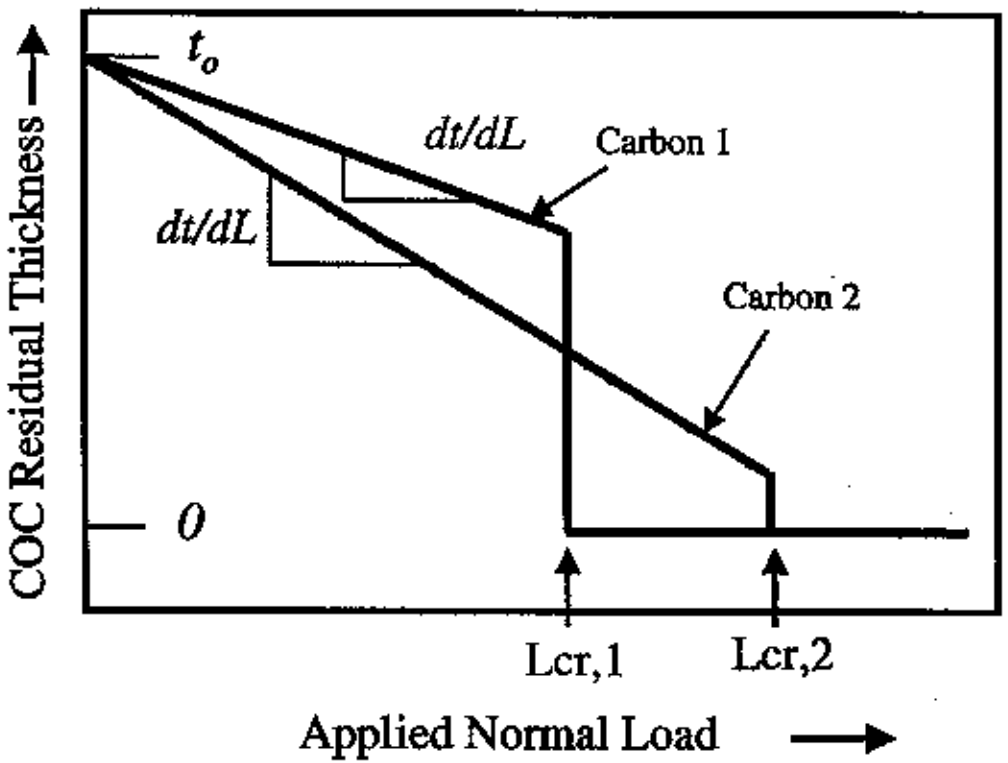
COC Residual Thickness
t_o
dt/dL
Carbon 1
dt/dL
Carbon 2
0
Lcr,1
Lcr,2
Applied Normal Load

Fig. 11